

## Article

# Impact of Fracture–Seepage–Stress Coupling on the Sustainability and Durability of Concrete: A Triaxial Seepage and Mechanical Strength Analysis

Zhuolin Shi <sup>1,2</sup>, Chengle Wu <sup>1,2</sup>, Furong Wang <sup>1,2</sup>, Xuehua Li <sup>1,2,\*</sup> , Changhao Shan <sup>1,2</sup> and Yingnan Xu <sup>1,2</sup>

<sup>1</sup> Key Laboratory of Deep Coal Resource Mining, Ministry of Education, School of Mines, China University of Mining and Technology, Xuzhou 221008, China

<sup>2</sup> School of Mines, China University of Mining and Technology, Xuzhou 221116, China

\* Correspondence: xuehua\_cumt@163.com

**Abstract:** As an indispensable material in construction and engineering, concrete's mechanical properties and permeability are crucial for structures' stability and durability. In order to reasonably assess and improve the durability of fracture-containing concrete structures and to enhance the sustainable working life of concrete structures, this research investigated the seepage characteristics of fracture-containing concrete and its mechanical property deterioration under fracture–seepage coupling by testing the permeability and strength of concrete samples before and after water penetration using triaxial seepage test and mechanical strength test. The results show that the fracture–seepage coupling action significantly affects the permeability characteristics and mechanical strength of fracture-containing concrete. In particular, the strength of concrete samples containing a single fracture decreased with increased fracture angle, with a maximum decrease of 32.8%. The fracture–seepage–stress coupling significantly reduced the strength of the fracture-containing concrete samples, which was about twice as much as the strength of the no-fracture concrete samples. Different fracture angles affect the mode of fracture expansion and damage (The fracture angle varies from small to large, and the damage form of concrete changes from tensile damage to tensile–shear composite damage). Moreover, the coupling effect of fracture–seepage–stress will further increase fracture-containing concrete's fragmentation in the damage process. Therefore, improving the seepage and fracture resistance of concrete plays a vital role in improving the sustainable working life of concrete structures.

**Keywords:** mechanical properties; durability; fracture-containing concrete; seepage characteristics; fracture–seepage coupling



**Citation:** Shi, Z.; Wu, C.; Wang, F.; Li, X.; Shan, C.; Xu, Y. Impact of Fracture–Seepage–Stress Coupling on the Sustainability and Durability of Concrete: A Triaxial Seepage and Mechanical Strength Analysis. *Sustainability* **2024**, *16*, 1187. <https://doi.org/10.3390/su16031187>

Academic Editors: Mahdi Kioumarsi and Vagelis Plevris

Received: 2 January 2024

Revised: 25 January 2024

Accepted: 28 January 2024

Published: 31 January 2024



**Copyright:** © 2024 by the authors. Licensee MDPI, Basel, Switzerland. This article is an open access article distributed under the terms and conditions of the Creative Commons Attribution (CC BY) license (<https://creativecommons.org/licenses/by/4.0/>).

## 1. Introduction

### 1.1. Importance of Concrete and Its Strength: Seepage Characteristics

Concrete, as an important material in construction and engineering, is widely used in the building industry and underground engineering. Investigating the permeability and mechanical properties of concrete with fracture is essential to improve the sustainable use of concrete in buildings and extend its service life. An in-depth understanding of the effect of fracture on the permeability and strength of concrete can help design structures with better durability, which can effectively prevent internal corrosion and deterioration, thus significantly improving the safety and stability of buildings. Such research can also facilitate the development of new durable concrete materials, further promoting concrete development for buildings towards sustainability and long life. While in working conditions, concrete is mainly subjected to pressure, so compressive strength becomes an important consideration in engineering design. With the complexity of the stress situation of concrete structure, in the actual project, concrete components will be affected by many uncertain factors (such as impact loading, temperature, construction technology, etc.) and produce different forms of fracture defects inside. Concrete structures are in long-term

working conditions with internal fractures. These fractures will further develop and expand under external stresses. This will reduce the durability and bearing capacity of the structure and accelerate its destruction. For example, in 2007, in Minneapolis, Minnesota, United States of America, the Highway 35 bridge collapsed as a result of a severe weakening of the concrete's load-bearing capacity due to long-accumulated cracks. This catastrophic event resulted in 13 deaths and some 145 injuries. The accident not only caused significant casualties and property damage but also raised widespread concerns about the safety and durability of infrastructure. Fractures in the concrete, in turn, create a large number of water-conducting channels. Underground structures such as tunnels, mining tunnels, and other critical large-scale projects such as dams, water surges in tunnels, tunnel collapses, and landslides are the leading causes of engineering safety accidents. Water penetrates the structure through the concrete matrix and internal fracture to damage the integrity and durability of the structure. In 2017, for example, a severe dam failure at the Oroville Dam in California, USA, was caused by seepage and erosion problems resulting from cracks in the dam's concrete structure. This resulted in the partial collapse of the dam's spillway and the emergency evacuation of nearly 188,000 residents, resulting in significant economic and social impacts.

In summary, the research on the degradation effect of fractures in concrete on the mechanical properties of concrete and the influence of concrete seepage characteristics is significant.

### *1.2. Progress of Research on the Effect of Fracture in Rock on the Strength of Concrete*

Some scholars [1–6] investigated single prefabricated fracture expansion patterns in rock materials under uniaxial loading. It was shown that multiple forms of secondary cracks would be generated at the tip of the prefabricated fracture in chronological order, and the expansion direction of the cracks was in the direction of the maximum principal stress. Yang et al. [7] obtained that fracture length and angle under axial pressure are the key influencing factors on the strength and deformation properties of sandstone samples by axial compression tests on single-fracture brittle sandstones. Qian et al. [8] analyzed the effect of fracture on the strength of rocks by axial compression tests on rock specimens. They concluded that the sensitivity of the factors influencing the strength of rocks is fracture filling, fracture angle, and fracture length, in descending order of magnitude. Chen et al. [9,10] investigated the effect of curing factors on the strength of concrete and the effect of chemical corrosion on the mechanical properties of concrete by triaxial mechanical tests. Xie et al. [11,12] used energy release and dissipation to determine the critical stress of the abrupt structural damage of rock samples under different stress states. Combined with CT scanning and acoustic emission, damage theory was introduced into analyzing damage mechanisms. Li et al. [13] investigated the crack extension damage evolution process by uniaxial compression test and CT scanning test of rocks. They concluded that the crack tip and edge are the cracking starting points of the fracture of rock samples. Lin et al. [14–16] investigated the expansion law of single fracture in mortar materials at different inclination angles. The results showed that when the angle between the fracture and the axial pressure direction was large, the cracks expanded unstably, and the samples were prone to cracking.

### *1.3. Progress of Seepage Characteristics of Fracture-Bearing Rock*

Regarding the research on the effect of fracture on the seepage characteristics of materials in rock materials, Bian et al. [17] investigated the evolution law of seepage properties in the water storage space of fractured sandstone in combination with in situ CT scanning technology. By using three-dimensional digital image technology, Chen et al. [18] investigated the mechanical model and the seepage characteristics of fracture in sandstone samples under different seepage pressures.

In general, although there has been extensive research on the mechanism of fracture extension, mechanical characteristic changes, and seepage evolution law of fracture-containing rock materials, there is less research on the related properties of concrete materi-

als. The effects of fractures in concrete and their comparison with the effects of fractures in rock materials are significantly different. In terms of differences in material properties, concrete is a composite material consisting of cement, sand, gravel, and water. This makes its internal structure and properties more complex than those of a single-component rock. Fracture extension in concrete is influenced by the interface between the aggregate and the cement paste. In terms of fracture generation and expansion, the formation of concrete fractures is influenced by various factors, such as loading, temperature changes, shrinkage, and corrosion. In contrast, rock fractures are usually caused by geological stresses, hydrogeological action, or external forces. In addition, fractures in concrete may extend gradually from microscopic defects. In contrast, macroscopic stress fields may affect rock fractures more directly. In terms of permeability differences, fractures in concrete usually affect its permeability, which is critical to the durability of the structure. The permeability of rock, on the other hand, is more influenced by the fracture system, and its permeation paths and rates differ significantly from those of concrete. The mechanical properties and seepage characteristics of concrete with fracture in actual engineering often determine the durability of concrete structures.

In this research, the permeability of concrete samples containing prefabricated fracture was obtained by conducting percolation tests on concrete samples under different triaxial stresses. In this way, the effects of different fracture morphologies (single fracture, Y-fracture, and X-fracture), fracture angle, and stress conditions on the percolation pattern of concrete samples were investigated. The strength decay characteristics of concrete strength under fracture–seepage coupling under different fracture morphology, fracture angle, and other conditions were investigated by conducting strength tests on fracture-containing concrete samples before and after seepage. Through this research, we can predict and respond more accurately to the effects of fracture on concrete performance so that measures can be taken at the design and construction stages to enhance the resistance to fracture and seepage of concrete structures. This is of great significance in improving the overall performance of buildings, extending their service life, and reducing the need for maintenance and repair at a later stage. Therefore, this research significantly impacts the promotion of concrete structures to be more sustainable and durable.

## 2. Experiment Preparation and Experimental Program Design

### 2.1. Sample Preparation

According to the sample size criteria recommended by the International Society for Rock Mechanics (ISRM) [19], cylindrical samples with dimensions  $\phi = 50$  mm and  $H = 100$  mm will be used in this research. This sample size is characterized by good uniformity, easy handling, and uniform stress distribution. Moreover, this sample size is consistent with the sample size in the international test method, and the experimental results obtained are also convenient for academic research and communication. The prepared fracture-containing concrete samples were made from concrete poured in advance and finished curing. The ratio of cement:sand:water:coarse sand in the concrete samples was 1:2:0.6:2, in which natural river sand was chosen as the concrete aggregate. Because of its uniform particle size and hardness, it can ensure the strength and compactness of the concrete sample. They were pouring concrete samples through molds. The concrete was vibrated using a vibrating table to remove internal gases and to compact the concrete. The poured concrete samples need to be cured at a temperature of about 24 °C and in 80–90% humidity. The concrete under cover should also be covered to prevent it from drying out too quickly. After 28 days of curing, the concrete samples with prefabricated single fracture, prefabricated Y-fracture, and prefabricated X-fracture were obtained by wire cutting. The sample preparation is shown in Figure 1. The concrete samples with a precast fracture are shown in Figure 2.

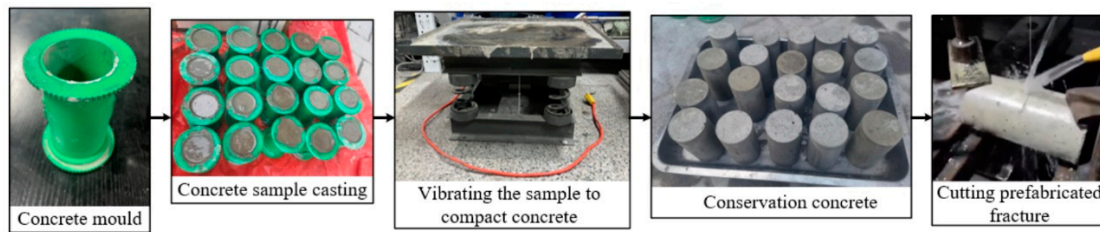


Figure 1. Sample preparation.

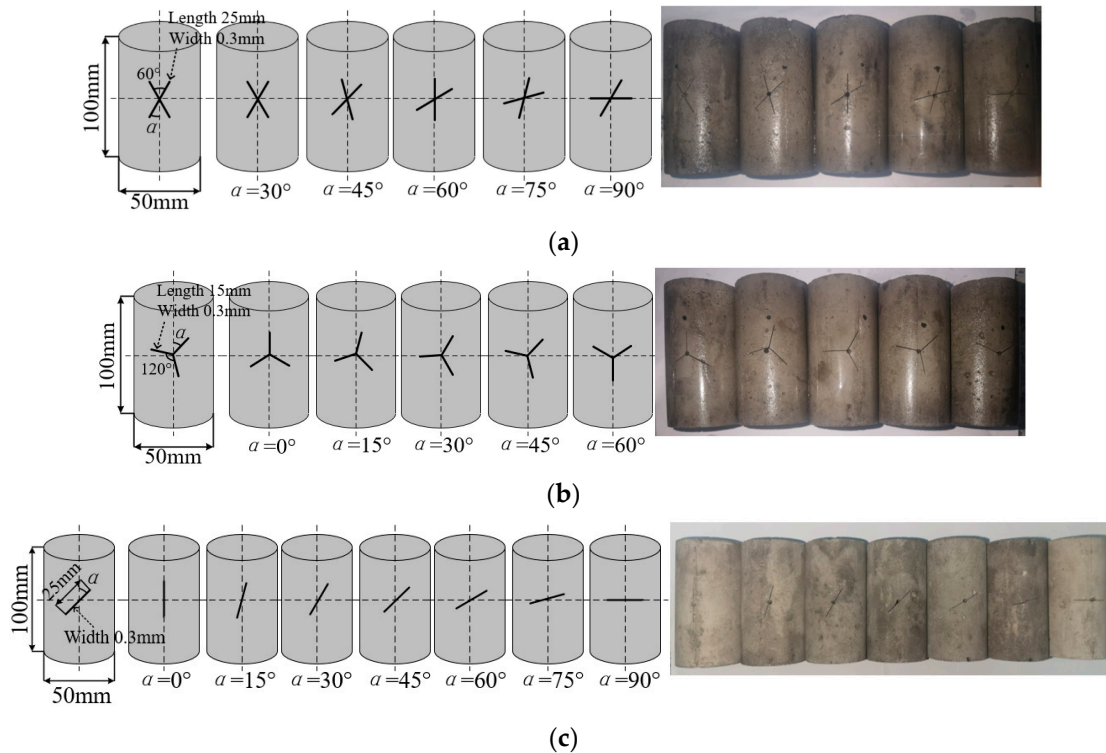
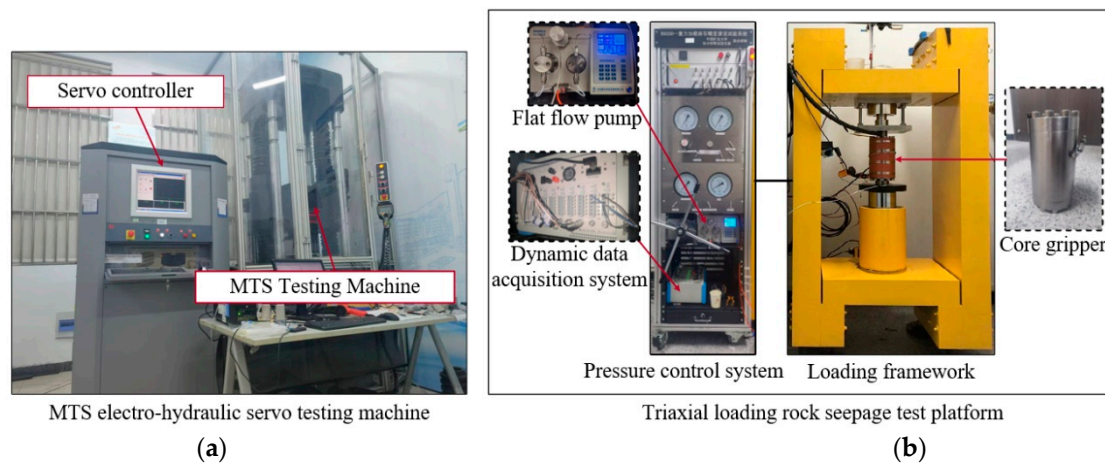


Figure 2. Concrete samples containing precast fractures: (a) X-fracture, (b) Y-fracture, and (c) single fracture.

## 2.2. Experimental Equipment

MTS electro-hydraulic servo testing machine was selected for mechanical characterization of concrete samples with fracture. The stress–strain curves and strengths of concrete samples before and after seepage under different fracture morphologies obtained from experiments can be analyzed to obtain the strength decay characteristics of fracture-containing concrete samples under fracture–seepage coupling.

The triaxial-loading rock-seepage test platform was selected for the test of seepage characteristics of concrete samples with fracture. The mass of outflow water per unit of time under different stress conditions can be obtained by applying different stresses to fracture-containing concrete samples using the seepage experimental platform. The permeability of the concrete samples can then be calculated to characterize the seepage properties of the concrete samples under different fracture patterns and stress conditions. The test platform consists of a load-bearing system, a loading system, a temperature control system, a seepage system, a measurement system, and an automatic acquisition and control system. In the loading system, the axial load  $\sigma_{1,\max} = 300$  kN, radial load  $\sigma_{2,\max} = \sigma_{3,\max} = 25$  MPa, and the upstream pressure of liquid seepage in the seepage system  $p_{w,\max} = 20$  MPa. The experimental equipment is shown in Figure 3. Among them, the principle of the triaxial-loading rock-seepage test platform is shown in Figure 4.



**Figure 3.** Experimental equipment: (a) MTS electro-hydraulic servo testing machine and (b) triaxial-loading rock-seepage test platform.

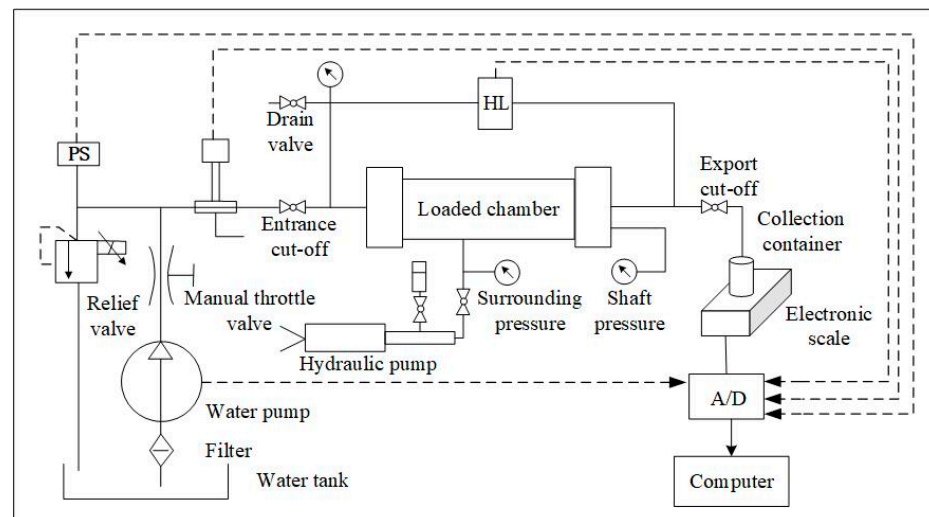


**Figure 4.** Principle of the triaxial-loading rock-seepage test platform.

### 2.3. Experimental Program

In natural rock and artificial concrete structures, fracture patterns are very complex. However, most complex fractures can be regarded as a combination of single fracture and cross-fracture. In order to investigate the effects of different fracture morphologies on the seepage characteristics and mechanical properties of concrete, single fracture, Y-fracture, and X-fracture are selected as the fracture morphologies to be studied in this research. In order to investigate the effect of concrete fracture on the seepage characteristics of concrete, seepage experiments were carried out on fracture-containing concrete samples using a triaxial-loading rock-seepage testing platform. The specific parameters of the fracture are shown in Figure 2. The experiments were conducted using concrete sample fracture morphology, fracture inclination, and external loading applied to the sample as the research variables. The experiment was conducted using stress-controlled loading, with axial stress  $\sigma_1$  and radial stress  $\sigma_2$  ( $\sigma_3$ ) applied at a rate of 1 MPa/min for preloading. Once the surrounding pressure reached the predetermined value of the experimental program, the surrounding pressure was kept constant, and the axial pressure was applied to the predetermined value of the experimental program. Keeping the axial stress  $\sigma_1$ , radial stress  $\sigma_2$ , and  $\sigma_3$  stable, the percolation pressure  $P_w$  was applied through an advection pump, and percolation was carried out using a constant flow pattern of 5 mL/min. Based on

the strength of the concrete samples in the pre-test and the equipment parameters, the experimental program in this research is shown in Table 1.

**Table 1.** Loading scheme for seepage test of concrete with fracture.

No.	Fracture Morphology	Fracture Angle/°	Surrounding Stress $\sigma_2$ ( $\sigma_3$ )/MPa	Axial Stress $\sigma_1$ /MPa	Seepage Stress $P_w$ /MPa
1	Without fracture	/			
2	Single fracture	0, 15, 30, 45, 60, 75, 90	4, 5, 6	6, 7, 8	3
3	Y-fracture	0, 15, 30, 45, 60			
4	X-fracture	30, 45, 60, 75, 90			

In the research, the effect of prefabricated fractures on the mechanical strength of concrete can be obtained by conducting compressive strength tests on concrete samples with single fracture, “Y” fracture, and “X” fracture with different inclination angles. The effect of fracture–seepage–stress coupling on the deterioration in the mechanical properties of concrete was investigated by conducting compressive strength tests on concrete samples after seepage tests and without seepage tests, respectively.

Under different seepage pressures and external stresses, fractured concrete’s fracture and microcrack morphology will change. Seepage water and external stresses also affect the microstructure of concrete and, hence, its water absorption. Therefore, concrete samples’ water absorption must be tested before starting the subsequent study. The saturated water content of the concrete samples before and after the percolation test was obtained by immersion testing of dry concrete samples to investigate the water absorption characteristics of the fractured concrete samples under seepage–stress coupling.

### 3. Characteristics of Seepage in Fracture-Containing Concrete

#### 3.1. Investigation of Water Absorption Characteristics of Fracture-Containing Concrete Samples under Seepage–Stress Coupling

A non-destructive water immersion device was used to saturate the samples. The water content of the concrete sample at the current moment was calculated by Equation (1).

$$w_t = \frac{m_t - m_s}{m_s} \times 100\% \quad (1)$$

where  $w_t$  is the moisture content of the sample after immersion time  $t$  expressed as %;  $m_t$  is the total mass of the sample after immersion time in g; and  $m_s$  is the mass of the sample when dry in g.

The average water content–time relationship of the fracture-containing concrete samples before and after the percolation experiment is shown in Figure 5.

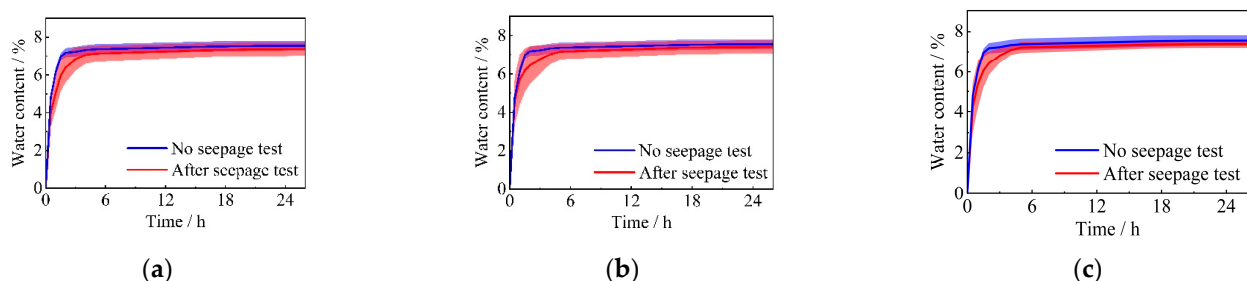


**Figure 5.** Mean moisture content–time relationship for concrete samples with fractures: (a) single fracture, (b) Y-fracture, and (c) X-fracture.

According to Figure 5, the average saturated water content of concrete samples without the percolation experiment is about 7.54%—the average saturated water content of concrete samples after the reduced percolation experiment. The average saturated water

content of concrete samples with a single fracture is about 7.37%, about 2.25% lower. The average saturated water content of concrete samples with Y-fracture is about 7.40%, about 1.86% lower. The average saturated water content of concrete samples with X-fracture is about 7.38 percent, about 2.12 percent lower. Concrete samples without percolation experiments reach 95% of the saturated water content in about 2 h. The time to reach saturated water content was prolonged for all the concrete samples containing fractures after the percolation experiment (single fracture, 4 h; Y-fracture, 4.5 h; and X-fracture, 4.5 h). From the microstructural aspect of the concrete samples, it is possible that the pore structure of the concrete was adjusted by the coupling of stress and seepage. The internal pores of concrete are reduced due to external stresses and seepage stresses. The capillary action of the concrete pores is reduced so that the water absorption efficiency of the sample is reduced, the saturated water content is reduced, and the time to reach the saturated state is prolonged. The presence of fracture reduces the saturated water content of concrete. This also provides additional space and channels for seepage, allowing water to penetrate deeper into the concrete. Moreover, due to the fracture in the sample, the stress concentration phenomenon occurs near the fracture of the sample when the external stress is applied. This stress concentration phenomenon causes the fracture to expand and change the water absorption channel, thus affecting the water absorption characteristics of concrete containing fractures. The prolonged percolation may also lead to changes in the internal microstructure of the concrete, such as stripping the aggregate–cement paste interface. These changes may also further affect the water absorption properties of concrete.

From the distribution of error bands in Figure 5, it can be seen that with the complexity of the geometrical characteristics of the fracture in the concrete sample (single fracture–Y-fracture–X-fracture), the water absorption characteristics of the concrete sample tend to stabilize (the width of the error band of the average water content gradually decreases). Comparing the error bands of concrete samples with the same fracture morphology before and after percolation, it can be seen that the water absorption characteristics of concrete changed significantly after percolation, and there are apparent differences in the water content state between samples at different times. The significant difference in the error bands of concrete samples with different fracture patterns before and after percolation also reflects the significant effect of fracture–seepage coupling on the water absorption of concrete. The range of the error bands can also reflect the permeability changes in concrete samples with different fracture patterns to a certain extent.

### 3.2. Seepage Characteristics of Concrete Samples Containing Fractures

Further investigation of the seepage characteristics of concrete samples can better reveal how water is transported along the fracture in fracture-containing concrete and how this process is affected by the external stress conditions of the concrete. Combined with the results of its water absorption characteristics, it can better help us to analyze the mechanical characteristics of fracture-containing concrete under complex environmental conditions. Fracture size, fracture angle, and fracture morphology are important fracture parameters that affect the seepage characteristics of concrete. Among them, previous research has explored the effect of rock fracture size on the seepage characteristics of rock and found that the rough fracture seepage of rock has an apparent size effect [20]. Next, the effect of fracture angle and fracture morphology on the seepage characteristics of fracture-containing concrete samples will be investigated. According to Darcy's law [21], a linear relationship exists between the seepage velocity of the fluid and the hydraulic gradient, as shown in Equation (2).

$$Q = k \frac{\Delta p A}{\mu l} \quad (2)$$

where  $Q$  is the fluid flow rate through the sample per unit time in  $\text{cm}^3/\text{s}$ ;  $k$  is the permeability of the sample in  $\text{m}^2$ ;  $A$  is the cross-sectional area of the fluid through the sample in  $\text{cm}^2$ ;  $\mu$  is the viscosity of the fluid in  $\text{Pa}\cdot\text{s}$ ;  $l$  is the length of the seepage path in  $\text{cm}$ ; and  $\Delta p$  is the pressure difference before and after the passage of the fluid through the sample in  $\text{MPa}$ .

The permeability  $k$  of the sample can be obtained according to Equation (3).

$$k = \frac{q\mu l}{\Delta p} \quad (3)$$

where  $q$  is the seepage velocity in cm/s.

The permeabilities of single-fracture concrete samples with different fracture angles under different stresses can be obtained from the seepage test of fracture-containing concrete samples, as shown in Figure 6. With the gradual increase in the angle between the fracture and the direction of seepage in the concrete samples, the permeability of concrete samples under each stress decreases. Among them, the permeability change was most evident in the fracture angle from  $0^\circ$  to  $30^\circ$ . As an example, when the surrounding pressure is 4 MPa and the axial pressure is 6 MPa, the permeability of the concrete sample decreases from  $6.46 \times 10^{-16} \text{ m}^2$  to  $2.87 \times 10^{-16} \text{ m}^2$ , which is a decrease of about 55.57% when the fracture angle in the concrete is increased from  $0^\circ$  to  $30^\circ$ . Throughout the process of increasing the fracture angle from  $0^\circ$  to  $90^\circ$ , the permeability of the concrete samples decreased from  $6.46 \times 10^{-16} \text{ m}^2$  to  $1.73 \times 10^{-16} \text{ m}^2$ , a decrease of about 73.22%. It can be seen that the permeability of concrete samples containing a single fracture is more significantly affected by the angle between the single fracture and the direction of seepage. The existence of fracture in the concrete sample shortens the distance of water seepage in its interior, so the sample's permeability is more significant when the angle between the single fracture and the seepage direction is minor. According to Figure 6, it can be seen that the permeability of concrete samples containing fractures is mainly affected by the stress perpendicular to the seepage direction. Due to the effect of stress perpendicular to the direction of seepage, the internal fracture and pore space of concrete is closed by pressure so that the seepage channel is reduced, which reduces the permeability of concrete samples. Moreover, this effect is more significant at low stress. Taking  $\sigma_1 = 6 \text{ MPa}$  as an example, when  $\sigma_2$  ( $\sigma_3$ ) increased from 4 MPa to 6 MPa, the permeability of concrete samples decreased by about 34.84% on average. Moreover, when  $\sigma_1 = 8 \text{ MPa}$ , the average decrease in permeability of concrete samples under the same condition is about 29.13%.

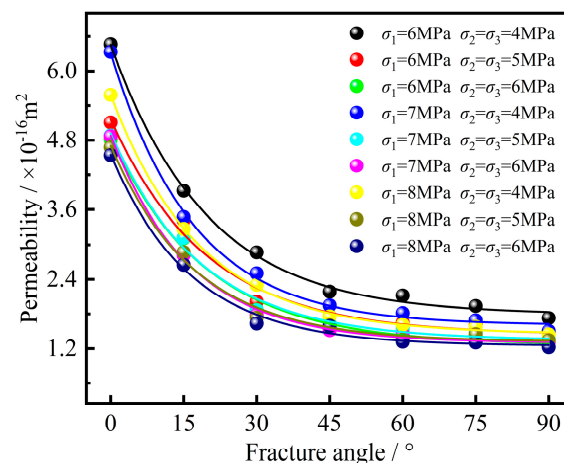
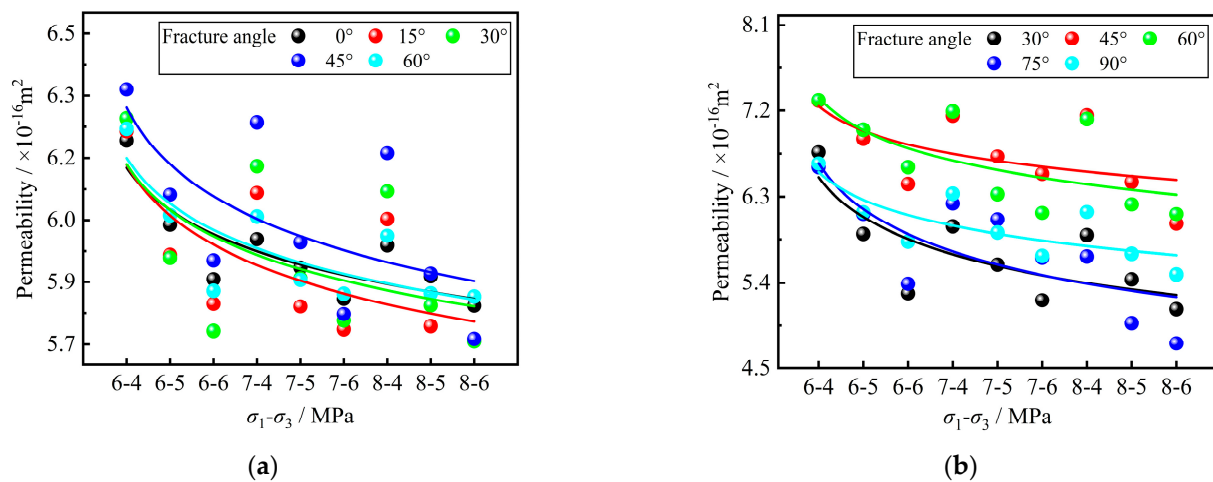


Figure 6. Permeabilities of single-fracture concrete samples with different fracture angles.

The permeabilities of Y-fracture and X-fracture concrete samples at different stresses are shown in Figure 7. Compared with the permeability change in concrete samples containing a single fracture at different fracture angles in Figure 6, the fracture angle does not significantly affect the permeability of concrete samples with Y-fracture and X-fracture. Taking the average permeability of concrete samples at each stage during the seepage experiments as an example, the average permeability of single-fracture concrete samples was reduced from  $3.03 \times 10^{-16} \text{ m}^2$  to  $2.04 \times 10^{-16} \text{ m}^2$ , a reduction of about 32.67%, during the process of increasing the stresses applied to the samples from  $\sigma_1 = 6 \text{ MPa}$  and  $\sigma_2$  ( $\sigma_3$ ) = 4 MPa to

$\sigma_1 = 8$  MPa and  $\sigma_2$  ( $\sigma_3$ ) = 6 MPa. The average permeability of Y-fracture concrete samples was reduced from  $6.24 \times 10^{-16} \text{ m}^2$  to  $5.75 \times 10^{-16} \text{ m}^2$ , about 7.85%. The average permeability of X-fracture concrete samples was reduced from  $6.73 \times 10^{-16} \text{ m}^2$  to  $5.65 \times 10^{-16} \text{ m}^2$ , about 16.05%. From the above, it can be seen that with the increase in the axial pressure and the surrounding pressure, the permeability of Y-fracture and X-fracture with different fracture angles shows an overall decreasing trend. From the analysis of fracture morphology, it can be seen that the more complex the fracture morphology is under the same stress condition, the smaller the effect of stress on the permeability of concrete samples. This suggests that a complex fracture structure may produce more seepage paths, thus reducing the effect of stress on permeability. In the seepage experiments, the average permeability of the concrete samples containing a single fracture was  $2.40 \times 10^{-16} \text{ m}^2$ , the average permeability of the concrete samples containing a Y-fracture was  $5.93 \times 10^{-16} \text{ m}^2$ , and the average permeability of the concrete samples containing an X-fracture was  $6.16 \times 10^{-16} \text{ m}^2$ . The more complex the fracture morphology of the concrete samples, the greater the permeability of the concrete samples. This also indicates that the complex fracture structure provides more channels for water seepage and increases the permeability of the concrete samples.



**Figure 7.** Permeabilities of concrete samples with complex fractures at different fracture angles: (a) Y-fracture and (b) X-fracture.

#### 4. Degradation of Mechanical Properties of Fracture-Containing Concrete

By exploring the effect of fracture–seepage–stress coupling on the strength of concrete, it is possible to reveal the specific effect of its complex coupling on the bearing capacity of concrete. Secondly, by investigating the damage characteristics of concrete, a more comprehensive understanding of the effects of different conditions on concrete can be obtained. The above research can provide a theoretical basis for better predicting and improving concrete performance and durability.

##### 4.1. Effect of Fracture–Seepage–Stress Coupling on the Strength of Concrete

Formation and development of fracture are the primary manifestations of concrete deterioration [22–24]. Fractures increase the stress concentration in concrete. The local stress concentration due to stress redistribution, in turn, promotes the generation of new fractures or the extension of existing ones, which reduces the overall load-bearing capacity of the concrete structure and reduces its strength [25]. Seepage of water and other fluids through concrete fracture may lead to chemical erosion or physical stripping of materials around concrete fracture [26–28]. This may lead to further expansion of the fracture in the concrete. At the same time, seepage’s physical erosion effect may change the concrete’s microstructure. This will increase the brittleness and reduce the strength of concrete to some extent. Different stress states may change the opening and direction of expansion and development of concrete fracture, thus affecting the permeability and mechanical

properties of concrete. It can be seen that stress redistribution, seepage erosion, and stress action generated by fracture have apparent effects on the mechanical properties of concrete. However, there is less research on coupling fracture, seepage, and stress. In general, the research on the effect of fracture–seepage–stress coupling on the strength of concrete is of great significance.

#### 4.1.1. Deterioration in Concrete Strength by Fractures in Concrete

The stress–strain curves of the fracture-containing concrete samples without the seepage test are shown in Figure 8. The strength of the concrete sample without fracture is about 14.15 MPa. The strength of the concrete sample with a single fracture is about 11.16 MPa, which is 21.13% lower than that of the concrete sample without fracture. The strength of the concrete sample with Y-fracture is about 9.01 MPa, which is 36.33% lower than that of the concrete sample without fracture. The strength of the concrete samples containing X-fracture is about 9.48 MPa, which is 33.00% lower than those without fracture. It can be seen that fracture in concrete has a more significant deteriorating effect on the strength of concrete. The existence of the fracture leads to the stress concentration phenomenon in concrete, which makes the local area of concrete reach the destructive strength earlier. The Y- and X-fractures, due to their more complex structure, produce a more obvious stress concentration at the tip of the fracture, leading to further degradation of the strength of the concrete samples. From the figure, it can also be found that the peak strain of the concrete samples decreases under the influence of the deteriorating effect of the fracture. The more complex the fracture morphology, the smaller the peak strain of concrete samples. During the compression process of the sample, there is a prominent stage of fracture closure in the concrete samples containing fracture, which is manifested by the rapid change in the stress–strain curve of the sample on the strain axis within a short period. The more complex the fracture morphology in the sample, the earlier the fracture closure phenomenon occurs. This also indicates that the deterioration effect of cracks in concrete samples is more apparent when the fracture morphology is more complex.

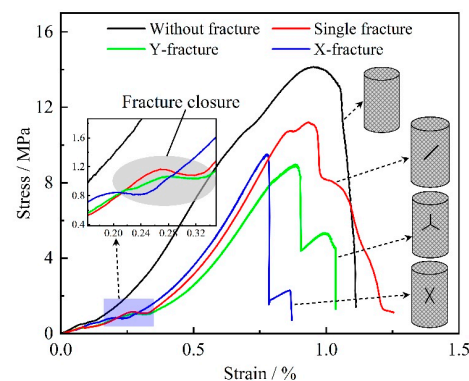


**Figure 8.** Stress–strain curves of fracture-containing concrete samples without seepage test.

#### 4.1.2. Deterioration in Concrete Strength by Fracture–Seepage–Stress Coupling

The strengths of fracture-containing concrete samples after the seepage experiment are shown in Table 2. The relationship between the strength attenuation in concrete samples under the coupled action of fracture–seepage–stress and the angle of the fracture is shown in Figure 9. Table 2 and Figure 9 show that different fracture morphologies will cause the strength of concrete samples to be significantly attenuated after the combined action of seepage and stress. Among them, after the same seepage pressure and external stress, the average attenuation in the strength of concrete samples with a single fracture is 26.06%, the average attenuation in the strength of concrete samples with Y-fracture is 32.06%, and the average attenuation in the strength of concrete samples with X-fracture is 37.83%. The more complex the fracture morphology, the stronger the deterioration effect on the concrete strength under the combined effect of fracture–seepage–stress. From Figure 9, it can be seen

that there is a positive correlation between the strength attenuation in concrete samples containing a single fracture and the single-fracture angle. This may be because the increase in the single-fracture angle leads to an increase in the area of the fracture in the direction perpendicular to the loading direction. Under the same external stress, the effective bearing area of the concrete samples decreases, which leads to different degrees of attenuation in the strength of the concrete samples. In contrast, in relatively complex fracture morphology (X and Y shapes), there is no significant relationship between the strength attenuation in concrete samples and the fracture angle.

**Table 2.** Strengths of fracture-containing concrete samples after seepage experiments.

No.	Fracture Morphology	Fracture Angle/ $^{\circ}$	Strength Average/MPa	Strength Decay/%
A1	Without fracture	/	13.02	/
B1	Single fracture	0	10.89	16.36
B2		15	10.29	20.97
B3		30	9.87	24.19
B4		45	9.50	27.04
B5		60	9.18	29.49
B6		75	8.91	31.57
B7		90	8.75	32.80
C1	Y-fracture	0	8.06	38.10
C2		15	9.31	28.49
C3		30	9.41	27.73
C4		45	9.23	29.11
C5		60	8.22	36.87
D1	X-fracture	30	8.19	37.10
D2		45	8.27	36.48
D3		60	7.83	39.86
D4		75	7.93	39.09
D5		90	8.25	36.64

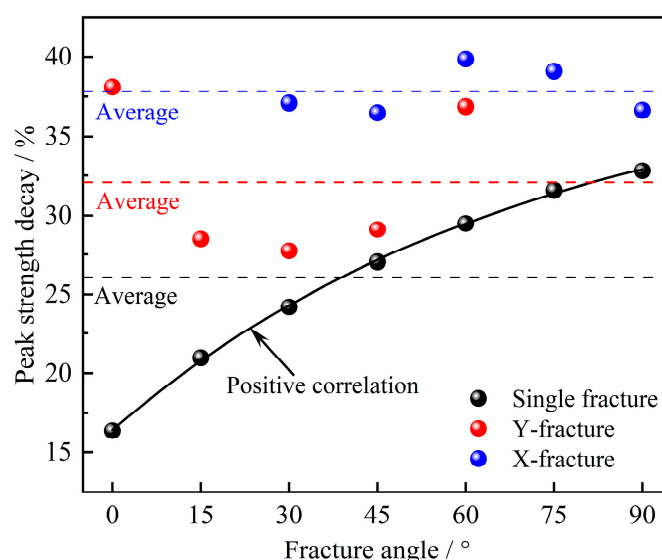


**Figure 9.** Strength decay of concrete samples under the coupled action of fracture–seepage–stress in relation to the angle of the fracture.

The average strengths of concrete samples before and after the seepage experiment are shown in Table 3. According to the data in the table, it can be seen that after the seepage experiment, the strength of concrete samples has different degrees of decline due to the joint effect of seepage and stress. Among them, the strength of concrete samples with fracture decreased significantly compared with that of concrete samples without fracture. Under the influence of seepage and stress, new microcracks may be generated around the cracks in the concrete samples, exacerbating the cracks' extension. Concrete samples with complex fractures may have more complex seepage channels, which may exacerbate the reduction in the load-carrying capacity of the samples after the seepage experiments. When there are fractures in concrete, the seepage medium (water) seeps through these channels. This seepage not only causes changes in pressure within the fracture. It also accelerates erosion within the concrete when the seepage medium contains chemicals that can react with the concrete components. All of these effects affect the development and expansion of microfractures in concrete. The presence of fracture reduces the overall continuity of concrete, making it more prone to fracture and damage under external stress. When the original fracture, seepage, and stress coupling will accelerate the expansion of secondary cracks, thus reducing the bearing capacity and durability of concrete. In general, the mechanical properties of concrete samples containing fractures will produce a more obvious deterioration phenomenon under fracture–seepage–stress coupling.

**Table 3.** Average strengths of concrete samples before and after seepage experiments.

Fracture Morphology	Average Strengths of Concrete Samples/MPa		Strength Decay/%
	No Seepage Experiment	After the Seepage Experiment	
Without fracture	14.15	13.02	7.99
Single fracture	11.16	9.50	14.87
Y-fracture	9.01	8.06	10.54
X-fracture	9.48	8.19	13.61

#### 4.2. Damage Characteristics of Fracture-Containing Concrete under Fracture–Seepage–Stress Coupling

##### 4.2.1. Characteristics of Crack Extension in Concrete with Fractures under Compression

In order to further clarify the damage characteristics of fracture-containing concrete, the crack extension characteristics of concrete samples with different fracture angles under compression after seepage tests are investigated. Currently, researchers have identified the types of cracks that can be observed in rock-like materials under uniaxial compression [29,30]. Under compression, wing cracks (smaller, spiky lateral cracks that accompany the main crack on either side) and secondary cracks (cracks initiated by extension of the main crack or stress concentration at the crack end) occur in rock-like materials [31]. Among them, wing cracks start to expand from the tip of the original fracture, which appears earlier. Moreover, it expands in a curvilinear path with increasing load. Wing cracks are a type of tensile crack, and the direction of initiation is approximately perpendicular to the direction of the original fracture. Secondary cracks appear later, usually in the form of shear cracks in the same plane of the original fracture expansion. According to the characterization of the crack surface, the crack form can be distinguished: wing cracks and tensile cracks have smooth surfaces. Secondary shear cracks (cracks that are perpendicular to the extension direction of the main crack and are in a shear state) have a rough surface accompanied by a large amount of rock particle debris. The shear strength can be characterized by the degree of debris fragmentation. A schematic diagram of the crack extension morphology and types of fracture-containing rock materials under compression is shown in Figure 10.

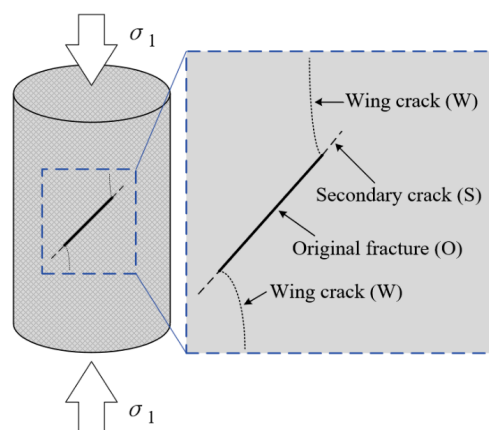


**Figure 10.** Morphology and type of crack extension after compression of fracture-containing rock-like materials.

Macroscopic crack expansion on the surface of concrete samples in various stages of compression was recorded by high-definition images. Now, the crack distribution images of each sample at the time of damage are taken to analyze the crack extension characteristics of the concrete containing fracture under compression. The crack expansion of concrete samples after compression damage is shown in Figure 11. In the compression process of the sample, the elastic deformation of concrete under compression led to the expansion of cracks. Moreover, the through fracture formed by the crack expansion led to the loss of bearing capacity and damage to the concrete sample. Wing cracks and secondary shear cracks mainly control the damage form of concrete samples. Among them, wing cracks initiate at the tip of the original fracture. When it expands to a certain extent, it will be connected to the secondary shear cracks generated from the end face of the sample, thus forming a through fracture between the end face of the sample and the original fracture, leading to the destruction of the sample.

According to the crack distribution of concrete samples under different fracture angles, it can be seen that the original fracture angle has different degrees of influence on the type of crack extension and final damage morphology of the samples. In concrete samples containing a single fracture, the macroscopic crack extension is more evident with increased fracture angle. Among them, when the fracture angle is slight, the damage form of the sample is dominated by tensile damage. When the fracture angle is larger, the damage form of the sample is dominated by tensile–shear composite damage. In the concrete samples containing Y-fracture or X-fracture, the influence of the fracture angle on the crack extension characteristics and the damage form of the sample is minor. According to the expansion of cracks in concrete samples with different fracture morphology, it can be seen that the more complex the original fracture morphology is, the more the number of wing cracks and secondary shear cracks produced by compression damage.

#### 4.2.2. Damage Fractals of Concrete Containing Fracture under Compression

The broken mass of concrete samples after destabilization and damage directly results from the extension and penetration of fractures and cracks, which has the value of fractal research [32]. The fractal research used the particle size–mass classification method to fractalize the broken blocks produced by compressing concrete samples containing fracture [33]. The broken masses of concrete samples were sieved using a particle-size sieve. The sieved particle size ranges were larger than 25 mm, 25–20 mm, 20–15 mm, 15–10 mm, 10–5 mm, 5–2.5 mm, and less than 2.5 mm, respectively. The sieved fractions of broken blocks of some concrete samples are shown in Figure 12.

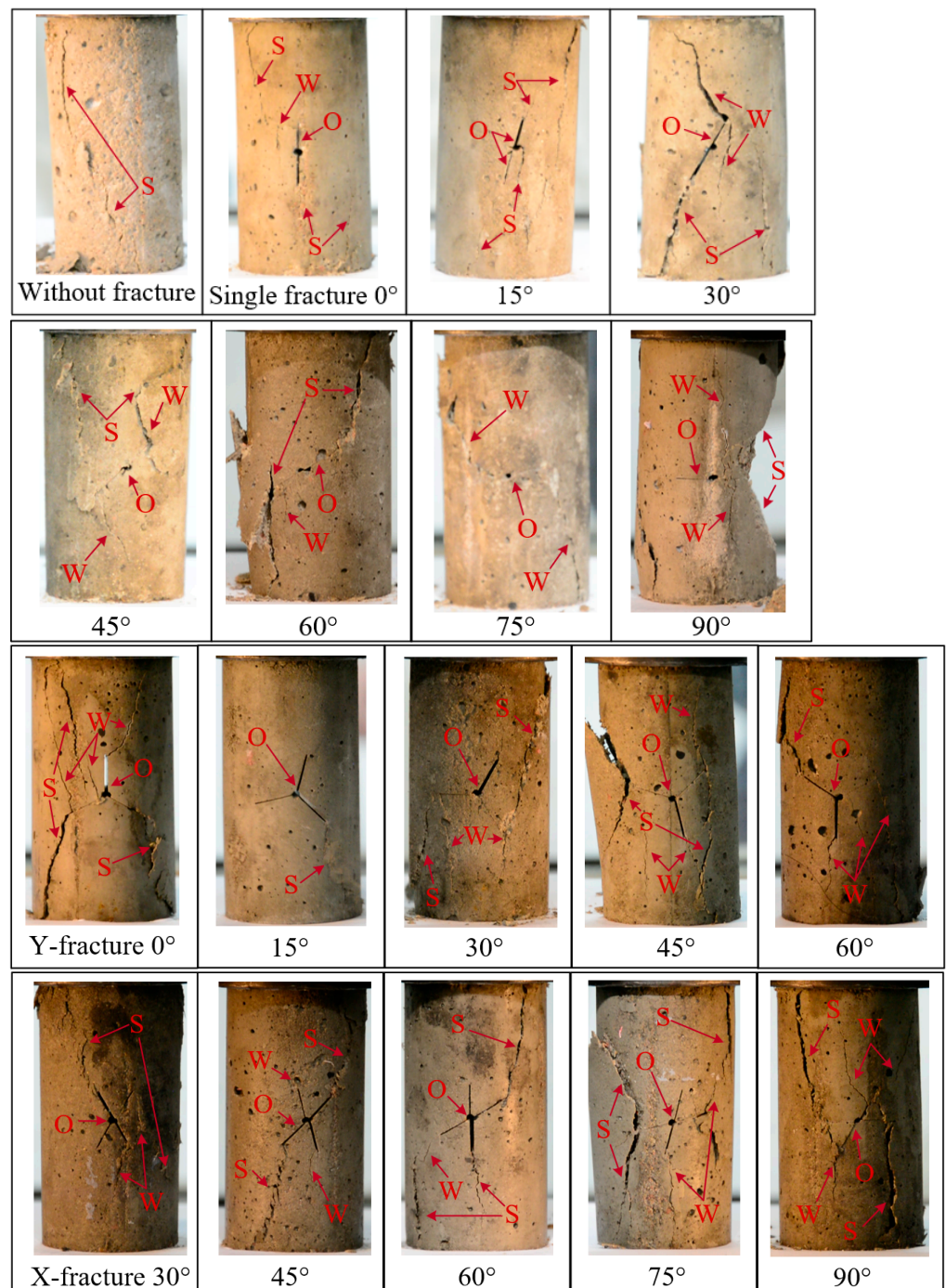


Figure 11. Expansion of cracks in concrete samples after damage under compression.

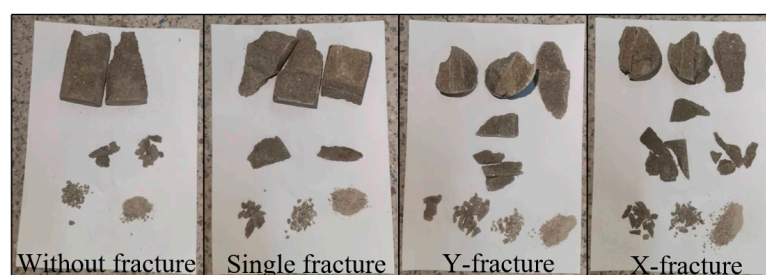


Figure 12. Sieving of broken masses of some concrete samples.

In this research, the mass of the broken mass  $M$  and the equivalent side length of the broken mass  $L_{eq}$  were used for statistical analysis to calculate the fractal dimension (a mathematical concept used to describe the complexity and irregularity of a rock's surface or internal structure) of the broken mass of the concrete sample  $D$ . The equations are as follows:

$$L_{eqi} = 1000 \cdot \sqrt[3]{\frac{m_i}{\rho \cdot 10^6}} \quad (4)$$

where  $L_{eqi}$  is the equivalent side length of the broken mass of the  $i$  sample in mm;  $\rho$  is the average density of the concrete sample in  $\text{kg}/\text{m}^3$ ; and  $m_i$  is the mass of the broken mass of the  $i$  sample in g.

$$\alpha = \frac{\lg(M_{L_{eq}}/M)}{\lg L_{eq}} \quad (5)$$

where  $\alpha$  is the slope of  $M_{L_{eq}}/M-L_{eq}$  in double logarithmic coordinates;  $M_{L_{eq}}/M$  is the cumulative percentage of fragments with equivalent side lengths less than  $L_{eq}$ ;  $M_{L_{eq}}$  is the mass of fragments corresponding to an equivalent side length of  $L_{eq}$  in g; and  $M$  is the total mass of fragments in the computational scale in g.

$$D = 3 - \alpha \quad (6)$$

The concrete sample broken-block mass–equivalent edge length relationships are shown in Figure 13. From the figure, it can be seen that the concrete sample broken-block mass–equivalent edge length has good linear correlation and self-similarity. It conforms to the fractal statistical distribution.

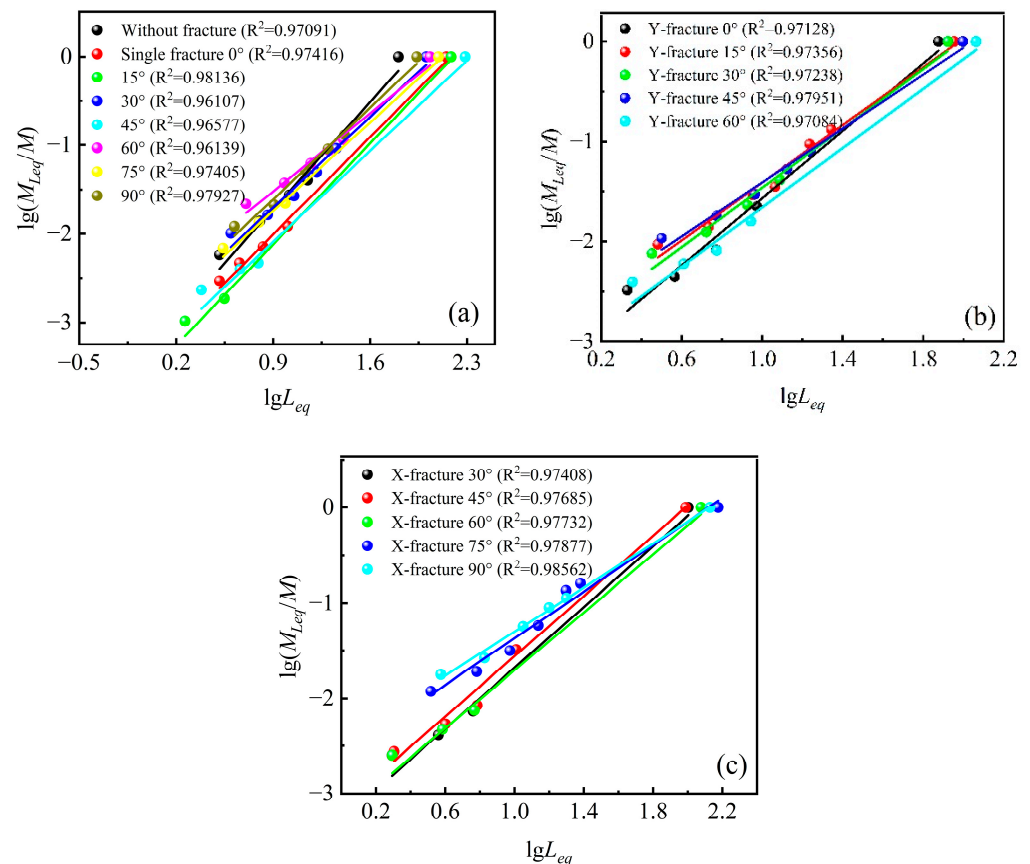


**Figure 13.** Mass–equivalent edge length relationships for broken blocks of concrete samples: (a) single fracture, (b) Y-fracture, and (c) X-fracture.

Statistically, the distribution of fractal dimensions of broken blocks of concrete samples in this research is shown in Figure 14. Concrete samples without fracture have the lowest fractal dimension, indicating that the structure of their broken blocks is relatively simple. The fractal dimension of concrete samples with a single fracture increased compared to the fractal dimension of concrete samples without fracture, indicating the effect of fracture on the structural complexity of the broken blocks of concrete samples. The fractal dimension of broken blocks of concrete samples further increased with the complexity of fracture morphology (Y-fracture and X-fracture). It can be seen that the presence and expansion of the fracture add new interfaces and discontinuities to the concrete sample on a macroscopic level. These fractures make the concrete sample more fragmented during compressive instability damage, producing broken blocks with smaller dimensions and less mass. A comparison of the fractal dimension of the broken blocks of concrete samples before and after the seepage experiments also shows a slight increase in the fractal dimension of the broken blocks of concrete samples after the seepage experiments. This may be related to the dynamic effect of fluid percolation. Under seepage and external stress, fracture-containing concrete's internal pore structure, microcrack, and stress state are redistributed. Moreover, this coupling effect will change the bond state inside the concrete, which reduces the strength of the concrete structure and causes more block fragmentation after damage.

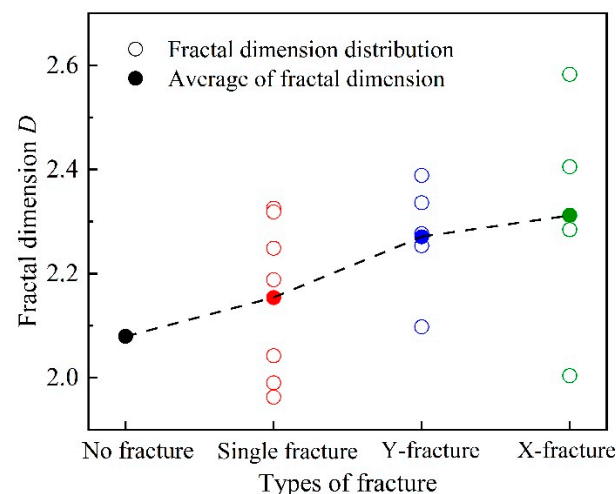


**Figure 14.** Distribution of fractal dimensions of broken blocks of concrete samples.

## 5. Conclusions

This research mainly carried out the seepage experiment and uniaxial compression test of concrete samples containing different fractures. It includes investigating the water absorption characteristics of concrete samples containing fractures, the change in permeability of samples under different stresses, and the mechanical strength and damage characteristics of samples with different fracture morphologies before and after the seepage experiments. Finally, the seepage characteristics of fracture-containing concrete under different stresses and the deterioration characteristics of mechanical properties of fracture-containing concrete under the action of fracture–seepage coupling were obtained. The main conclusions are as follows:

The action of seepage and external stresses can reduce the saturated water content of concrete and prolong the time it takes for the concrete to reach the saturated water content. The saturated water content is reduced by about 2.1%. In fracture-containing concrete, the stress concentration near the fracture will cause the fracture to expand and change the water-conducting channel. Therefore, the more complex the geometrical characteristics of the fracture in the concrete, the less time it takes for each concrete sample to reach saturation versus the change in saturated water content.

The permeability of concrete samples containing a single fracture decreases and stabilizes with the increase in the angle between the single fracture and the direction of seepage. Under the stress conditions of this research, the permeability of the concrete samples was reduced by about 73.2% when the pinch angle was 90° at maximum. However, in concrete with more complex fractures, the angle between the fracture and the seepage direction has no noticeable effect on the permeability of the concrete. The more complex fracture morphology can reduce the effect of stress on concrete permeability.

A single fracture in concrete samples reduces their strength with increasing angle between the fracture and the stress direction. More complex fracture morphology correlates with lower strength and peak strain. Seepage–stress coupling significantly affects strength, with fracture-containing samples experiencing double the strength decay compared to samples without fracture. Concrete samples with different fracture types also showed notable strength reductions, averaging 26.06% for single fracture, 32.06% for Y-fracture, and 37.83% for X-fracture.

The elastic deformation of concrete under compression is the leading cause of crack expansion in concrete samples, and crack development eventually leads to sample damage. The original fracture angle significantly affects the crack expansion and damage pattern. Smaller fracture angles in concrete samples with single fracture lead to tensile damage, and larger fracture angles lead to tensile–shear composite damage. The higher the complexity of the fracture morphology, the higher the number of wing cracks and secondary shear cracks generated during concrete damage, resulting in a more complex damage pattern. The fractal dimension of broken blocks of fracture-containing concrete samples increases with the complexity of fracture morphology. The coupling effect of fracture, seepage, and stress can further increase the fractal dimension of fracture-containing concrete broken blocks.

From the research on the effect of fracture–seepage–stress coupling on the strength and damage characteristics of concrete, it can be seen that the existence of fracture and its coupling with seepage and stress significantly reduces the bearing capacity and durability of concrete, which is manifested in the apparent deterioration in the mechanical properties of fracture-containing concrete after the occurrence of seepage phenomenon.

**Author Contributions:** Z.S., C.W. and X.L. conceived and designed the experimental program; Z.S., C.W. and F.W. derived the theoretical equations; Z.S., C.W., C.S. and Y.X. conducted the laboratory experiments; Z.S. and F.W. collated and analyzed the experimental data; Z.S. wrote the paper and X.L. helped Z.S. revise the manuscript. All authors have read and agreed to the published version of the manuscript.

**Funding:** This research was funded by the Science and Technology Innovation Special Fund of Jiangsu Provincial Science and Technology Department, approval No. BK20220024, project No. 2022-12460.

**Data Availability Statement:** No data were used to support this study.

**Conflicts of Interest:** The authors declare no conflicts of interest.

## References

1. Wei, C.; Zhang, B.; Zhu, W.; Wang, S.; Li, J.; Yang, L.; Lin, C. Fracture Propagation of Rock like Material with a Fluid-Infiltrated Pre-existing Flaw Under Uniaxial Compression. *Rock Mech. Rock Eng.* **2021**, *54*, 875–891. [[CrossRef](#)]
2. Nolen-Hoeksema, R.C.; Gordon, R.B. Optical detection of crack patterns in the opening-mode fracture of marble. *Int. J. Rock Mech. Min. Sci. Geomech. Abstr.* **1987**, *24*, 135–144. [[CrossRef](#)]
3. Van Mier, J.; Man, H.K. Some Notes on Microcracking, Softening, Localization, and Size Effects. *Int. J. Damage Mech.* **2009**, *18*, 283–309. [[CrossRef](#)]
4. Lajtai, E.Z. Unconfined Shear Strength of Discontinuous Rocks. In Proceedings of the 2nd ISRM Congress, Belgrade, Yugoslavia, 21–26 September 1970.
5. Feng, G.; Zhu, C.; Wang, X.; Tang, S. Thermal effects on prediction accuracy of dense granite mechanical behaviors using modified maximum tangential stress criterion. *J. Rock Mech. Geotech.* **2023**, *15*, 1734–1748. [[CrossRef](#)]

6. Feng, G.; Wang, X.C.; Kang, Y.; Zhang, Z.T. Effect of thermal cycling-dependent cracks on physical and mechanical properties of granite for enhanced geothermal system. *Int. J. Rock Mech. Min.* **2020**, *134*, 104476. [[CrossRef](#)]
7. Wong, R.; Lin, P.; Tang, C.A. Experimental and numerical study on splitting failure of brittle solids containing single pore under uniaxial compression. *Mech. Mater.* **2006**, *38*, 142–159. [[CrossRef](#)]
8. Qianqian, D.; Guowei, M.; Qiusheng, W.; Mingjie, X.; Qiaoyan, L. Different damage parameters on failure properties with non-straight marble under uniaxial compression. *Electron. J. Geotech. Eng.* **2015**, *20*, 6151–6167.
9. Chen, D.; Yu, X.; Liu, R.; Li, S.; Zhang, Y. Triaxial mechanical behavior of early age concrete: Experimental and modelling research. *Cem. Concr. Res.* **2019**, *115*, 433–444. [[CrossRef](#)]
10. Chen, D.; Yu, X.T.; Guo, M.Y.; Liao, Y.D.; Ouyang, F. Study on the mechanical properties of the mortars exposed to the sulfate attack of different concentrations under the triaxial compression with constant confining pressure. *Constr. Build. Mater.* **2017**, *146*, 445–454. [[CrossRef](#)]
11. Xie, H.P.; Yang, J.U. Criteria for Strength and Structural Failure of Rocks Based on Energy Dissipation and Energy Release Principles. *Chin. J. Rock Mech. Eng.* **2005**, *24*, 3003–3010.
12. Yuangao, L.; Weiyuan, Z.; Jidong, Z.; Qiang, Y. Discontinuous Bifurcation Model of Damage Localization for Jointed Rocks and its Application. *Acta Mech. Sin. Chin. Ed.* **2003**, *35*, 411–418.
13. Li, J.C.; Li, T.C.; Wang, G.; Bai, S.W. CT scanning test of built-in fracture extension under uniaxial compression. *J. Rock Mech. Eng.* **2007**, *26*, 484–492.
14. Wang, W.H.; Wang, X.J.; Jiang, H.T.; Yan, Z.; Li, S.R. Mechanical properties of rock-like samples with different inclination fracture under uniaxial compression. *Sci. Technol. Bull.* **2014**, *32*, 48–53.
15. Lin, P.; Huang, K.J.; Wang, R.K.; Zhou, W.Y. Crack extension and damage behaviour of samples with single crack defects at different angles. *J. Rock Mech. Eng.* **2005**, 5652–5657. Available online: [https://www.researchgate.net/publication/294743512\\_Crack\\_growth\\_mechanism\\_and\\_failure\\_behavior\\_of\\_specimen\\_containing\\_single\\_flaw\\_with\\_different\\_angles](https://www.researchgate.net/publication/294743512_Crack_growth_mechanism_and_failure_behavior_of_specimen_containing_single_flaw_with_different_angles) (accessed on 9 December 2023).
16. Xie, Q.T.; Guo, J.Z.; Wang, J.L.; Chen, Y.G. Crack extension measurement in sandstone specimens with inclined single cracks under uniaxial compression. *Geotechnics* **2011**, *32*, 2917–2921.
17. Bian, H.; Qin, X.W.; Luo, W.J.; Ma, C.; Zhu, J.; Lu, C.; Zhou, Y.F. Evolution of hydrate habit and formation properties evolution during hydrate phase transition in fractured-porous medium. *Fuel* **2022**, *324*, 124436. [[CrossRef](#)]
18. Chen, Y.; Xu, J.; Peng, S.J.; Zhang, Q.W.; Chen, C.C. Strain localisation and seepage characteristics of rock under triaxial compression by 3D digital image correlation. *Int. J. Rock Mech. Min.* **2022**, *152*, 105064. [[CrossRef](#)]
19. Hudson, J.A.; Cornet, F.H.; Christiansson, R. ISRM Suggested Methods for rock stress estimation—Part 1: Strategy for rock stress estimation. *Int. J. Rock Mech. Min.* **2003**, *40*, 991–998. [[CrossRef](#)]
20. Shi, Z.; Yao, Q.; Wang, W.; Su, F.; Li, X.; Zhu, L.; Wu, C. Size Effects of Rough Fracture Seepage in Rocks of Different Scales. *Water-Sui* **2023**, *15*, 1912. [[CrossRef](#)]
21. Gray, W.G.; Miller, C.T. Examination of Darcy's law for flow in porous media with variable porosity. *Environ. Sci. Technol.* **2004**, *38*, 5895–5901. [[CrossRef](#)]
22. Zhang, D.; Yao, H. Disease Analysis and solutions of the prestressed concrete bridge cracks. In Proceedings of the 2nd International Conference on Civil Engineering, Architecture and Building Materials (CEABM 2012), Yantai, China, 25–27 May 2012; Volume 178–181, pp. 2398–2400.
23. Shaikh, F.U. A Effect of Cracking on Corrosion of Steel in Concrete. *Int. J. Concr. Struct. Mater.* **2018**, *12*, 3. [[CrossRef](#)]
24. Combrinck, R.; Steyl, L.; Boshoff, W.P. Influence of concrete depth and surface finishing on the cracking of plastic concrete. *Constr. Build. Mater.* **2018**, *175*, 621–628. [[CrossRef](#)]
25. Yang, J.Y.; Guo, Y.C.; Tan, J.J.; Shen, A.Q.; Wu, H.; Li, Y.; Lyu, Z.H.; Wang, L.S. Strength deterioration and crack dilation behavior of BFRC under dynamic fatigue loading. *Case Stud. Constr. Mater.* **2022**, *16*, e01051. [[CrossRef](#)]
26. Ting, S.; Yang, L.; IOP. Chloride ion erosion experiment research in cracked concrete. In Proceedings of the 2nd International Conference on Materials Science, Energy Technology and Environmental Engineering (MSETEE), Zhuhai, China, 28–30 April 2017; Volume 81.
27. Gao, Y.; Zou, C. CT study on meso-crack propagation of gradient composite concrete subjected to sulfate erosion. *Mag. Concr. Res.* **2015**, *67*, 1127–1134. [[CrossRef](#)]
28. Guo, J.; Wang, K.; Guo, T.; Yang, Z.; Zhang, P. Effect of Dry-Wet Ratio on Properties of Concrete Under Sulfate Attack. *Materials* **2019**, *12*, 2755. [[CrossRef](#)] [[PubMed](#)]
29. Lee, J.; Hong, J.W. Morphological aspects of crack growth in rock materials with various flaws. *Int. J. Numer. Anal. Met.* **2019**, *43*, 1854–1866. [[CrossRef](#)]
30. Silva, B.G.D.; Einstein, H.H. Modeling of crack initiation, propagation and coalescence in rocks. *Int. J. Fract.* **2013**, *182*, 167–186. [[CrossRef](#)]
31. Rhc, W.; Kt, C. Crack coalescence in a rock-like material containing two cracks. *Int. J. Rock Mech. Min.* **1998**, *35*, 147–164.

32. Xie, H.P.; Gao, F.; Zhou, H.W.; Zuo, J.P. Fractal study of rock fracture and fragmentation. *J. Disaster Prev. Mitig. Eng.* **2003**, *1*–9. Available online: <https://kns.cnki.net/KXReader/Detail?invoice=Ytr/JrSeUr7dE1unRvbIcxIZDvXD4kYuSm/DvinUguvfj3BIAvt3a8sFLwvQnkEQIJeL2HXfbf5H4XGk/IHLW7aV2tVZZbJt9oq/pDGqplpJvrSjfRtwpK8L5bFcpXF9KqXdRZ72naQLGthNT5tNW2UwoXm24v+u7bTY77hhM=&DBCOD=CFJQ&FileName=DZXK200304000&TABLEName=cjfd2003&nonce=3AA62C61C3594E6A8D149487A5BD609B&TIMESTAMP=1706602578386&uid=> (accessed on 9 December 2023).
33. He, M.C.; Yang, G.X.; Miao, J.L.; Jia, X.N.; Jiang, T.T. Classification of debris in rock explosion experiments and its research method. *J. Rock Mech. Eng.* **2009**, *28*, 1521–1529.

**Disclaimer/Publisher’s Note:** The statements, opinions and data contained in all publications are solely those of the individual author(s) and contributor(s) and not of MDPI and/or the editor(s). MDPI and/or the editor(s) disclaim responsibility for any injury to people or property resulting from any ideas, methods, instructions or products referred to in the content.